2017

Introducing Global Peat-Specific Temperature and pH Calibrations Based on brGDGT Bacterial Lipids

B.D.A. Naafs

G. N. Imglis

Y. Zheng

M. J. Amesbury

H. Biester

See next page for additional authors

Repository Citation

Naafs, B.D.A.; Imglis, G. N.; Zheng, Y.; Amesbury, M. J.; Biester, H.; Bindler, R.; Blewett, J.; Burrows, M. A.; Torres, D. del Castillo; Chambers, F. M.; and Hatcher, P. G., "Introducing Global Peat-Specific Temperature and pH Calibrations Based on brGDGT Bacterial Lipids" (2017). *Chemistry & Biochemistry Faculty Publications*. 94.
https://digitalcommons.odu.edu/chemistry_fac_pubs/94

Authors

B.D.A. Naafs, G. N. Imglis, Y. Zheng, M. J. Amesbury, H. Biester, R. Bindler, J. Blewett, M. A. Burrows, D. del Castillo Torres, F. M. Chambers, and P. G. Hatcher

Introducing global peat-specific temperature and pH calibrations based on brGDGT bacterial lipids

B.D.A. Naafs [a,b,*], G.N. Inglis [a,b], Y. Zheng [c], M.J. Amesbury [d], H. Biester [e],
R. Bindler [f], J. Blewett [a,b], M.A. Burrows [g], D. del Castillo Torres [h],
F.M. Chambers [i], A.D. Cohen [j], R.P. Evershed [a,b], S.J. Feakins [k], M. Gałka [l],
A. Gallego-Sala [d], L. Gandois [m], D.M. Gray [n], P.G. Hatcher [o], E.N. Honorio
Coronado [h], P.D.M. Hughes [p], A. Huguet [q], M. Könönen [r], F. Laggoun-Défarge [s],
O. Lähteenoja [t], M. Lamentowicz [u], R. Marchant [v], E. McClymont [a,w], X. Pontevedra-
Pombal [x], C. Ponton [j], A. Pourmand [y], A.M. Rizzuti [z], L. Rochefort [aa],
J. Schellekens [ab], F. De Vleeschouwer [m], R.D. Pancost [a,b]

[a] Organic Geochemistry Unit, School of Chemistry, University of Bristol, Bristol, UK
[b] Cabot Institute, University of Bristol, Bristol, UK
[c] State Key Laboratory of Continental Dynamics, Department of Geology, Northwest University, Xi'an, PR China
[d] Geography, College of Life and Environmental Sciences, University of Exeter, Exeter, UK
[e] Institut für Geoökologie, AG Umweltgeochemie, Technische Universität Braunschweig, Braunschweig, Germany
[f] Department of Ecology and Environmental Science, Umeå University, Umeå, Sweden
[g] Australian National University, Acton, Canberra, Australia
[h] Instituto de Investigaciones de la Amazonía Peruana (IIAP), Iquitos, Peru
[i] Centre for Environmental Change and Quaternary Research, School of Natural and Social Sciences, University of Gloucestershire, Cheltenham, UK
[j] Department of Earth and Ocean Sciences, University of South Carolina, Columbia, USA
[k] Department of Earth Sciences, University of Southern California, Los Angeles, USA
[l] Department of Biogeography and Paleoecology, Adam Mickiewicz University in Poznań, Poznań, Poland
[m] ECOLAB, Université de Toulouse, CNRS, INPT, UPS, Toulouse, France
[n] Pinelands Field Station, Rutgers University, New Lisbon, USA
[o] Department of Chemistry and Biochemistry, Old Dominion University, Norfolk, USA
[p] Palaeoecology Laboratory, University of Southampton, Southampton, UK
[q] Sorbonne Universités, UPMC, Univ Paris 06, CNRS, EPHE, UMR 7619 METIS, Paris, France
[r] Department of Forest Sciences, University of Helsinki, Finland
[s] Université d'Orléans/CNRS/BRGM, ISTO, UMR 7327, Orléans, France
[t] Department of Biology, University of Turku, Finland
[u] Laboratory of Wetland Ecology and Monitoring & Department of Biogeography and Paleoecology, Adam Mickiewicz University in Poznań, Poznań, Poland
[v] York Institute for Tropical Ecosystems, Environment Department, Wentworth Way University of York, York, UK
[w] Department of Geography, Durham University, Durham, UK
[x] Departamento de Edafoloxía e Química Agrícola, Universidade de Santiago de Compostela, Santiago de Compostela, Spain
[y] Department of Marine Geosciences, University of Miami – RSMAS, Miami, USA
[z] Department of Chemistry, Claflin University, Orangeburg, USA
[aa] Peatland Ecology Research Group (PERG), Centre for Northern Studies, Université Laval, Quebec City, Canada
[ab] Department of Soil Science, University of São Paulo, Piracicaba, Brazil

* Corresponding author at: Organic Geochemistry Unit, School of Chemistry, University of Bristol, Bristol, UK.
  E-mail address: david.naafs@bristol.ac.uk (B.D.A. Naafs).

Abstract

Glycerol dialkyl glycerol tetraethers (GDGTs) are membrane-spanning lipids from Bacteria and Archaea that are ubiquitous in a range of natural archives and especially abundant in peat. Previous work demonstrated that the distribution of bacterial branched GDGTs (brGDGTs) in mineral soils is correlated to environmental factors such as mean annual air temperature (MAAT) and soil pH. However, the influence of these parameters on brGDGT distributions in peat is largely unknown. Here we investigate the distribution of brGDGTs in 470 samples from 96 peatlands around the world with a broad mean annual air temperature (−8 to 27 °C) and pH (3–8) range and present the first peat-specific brGDGT-based temperature and pH calibrations. Our results demonstrate that the degree of cyclisation of brGDGTs in peat is positively correlated with pH, $pH = 2.49 \times CBT_{peat} + 8.07$ ($n = 51$, $R^2 = 0.58$, RMSE = 0.8) and the degree of methylation of brGDGTs is positively correlated with MAAT, $MAAT_{peat}$ (°C) $= 52.18 \times MBT'_{5me} - 23.05$ ($n = 96$, $R^2 = 0.76$, RMSE = 4.7 °C). These peat-specific calibrations are distinct from the available mineral soil calibrations. In light of the error in the temperature calibration (∼4.7 °C), we urge caution in any application to reconstruct late Holocene climate variability, where the climatic signals are relatively small, and the duration of excursions could be brief. Instead, these proxies are well-suited to reconstruct large amplitude, longer-term shifts in climate such as deglacial transitions. Indeed, when applied to a peat deposit spanning the late glacial period (∼15.2 kyr), we demonstrate that $MAAT_{peat}$ yields absolute temperatures and relative temperature changes that are consistent with those from other proxies. In addition, the application of $MAAT_{peat}$ to fossil peat (i.e. lignites) has the potential to reconstruct terrestrial climate during the Cenozoic. We conclude that there is clear potential to use brGDGTs in peats and lignites to reconstruct past terrestrial climate.

1. INTRODUCTION

Although reconstructions of terrestrial environments are crucial for the understanding of Earth's climate system, suitable depositional archives (especially longer continuous sequences) are rare on land. Peatlands and lignites (naturally compressed ancient peat) are one exception and offer remarkable preservation of organic matter. Peats can be found in all climate zones where suitable waterlogged conditions exist. Typical peat accumulation rates are on the order of 1–2 mm/year (Gorham et al., 2003) and because they exhibit minimal bioturbation (although roots might be present) they are widely used as climate archives during the late Quaternary, predominantly the Holocene (e.g., Barber, 1993; Chambers and Charman, 2004). Peat-based proxies include those based on plant macrofossils, pollen, and testate amoebae (e.g., Woillard, 1978; Mauquoy et al., 2008; Väliranta et al., 2012), inorganic geochemistry (e.g., Burrows et al., 2014; Chambers et al., 2014; Hansson et al., 2015; Vanneste et al., 2015), (bulk) isotope signatures (e.g., Cristea et al., 2014; Roland et al., 2015) and organic biomarkers (e.g., Nichols et al., 2006; Pancost et al., 2007; Pancost et al., 2011; Huguet et al., 2014; Zocatelli et al., 2014; Schellekens et al., 2015; Zheng et al., 2015). Although these proxies can be used to provide a detailed reconstruction of the environment and biogeochemistry within the peat during deposition, an accurate temperature or pH proxy for peat is currently lacking (Chambers et al., 2012). This is particularly problematic because temperature and pH are key environmental parameters that directly affect vegetation type, respiration rates, and a range of other wetland features (e.g., Lafleur et al., 2005; Yvon-Durocher et al., 2014). The aim of this paper is to develop peat-specific pH and temperature proxies for application to peat cores as well as ancient peats from the geological record preserved as lignites.

We focus on using membrane-spanning glycerol dialkyl glycerol tetraether (GDGT) lipids. In general, two types of GDGTs are abundant in natural archives such as peats: (1) isoprenoidal (iso)GDGTs with 2,3-*sn*-glycerol stereochemistry that are synthesized by a wide range of Archaea, and (2) branched (br)GDGTs with 1,2-*sn*-glycerol stereochemistry that are produced by Bacteria (see review by Schouten et al., 2013 and references therein). A wide range of brGDGTs occur in natural archives such as mineral soils and peat; specifically, tetra-, penta-, and hexamethylated brGDGTs, each of which can contain 0, 1, or 2 cyclopentane rings (Weijers et al., 2006b). In addition, recent studies using peat and mineral soils have demonstrated that the additional methyl group(s) present in penta- and hexamethylated brGDGTs can occur on either the α and/or ω-5 position (5-methyl brGDGTs) or the α and/or ω-6 position (6-methyl brGDGTs) (De Jonge et al., 2013, 2014). brGDGTs are especially abundant in peat, in fact brGDGTs were first discovered in a Dutch peat (Sinninghe Damsté et al., 2000). The concentration of brGDGTs (as well as isoGDGTs) is much higher in the water saturated and permanently anoxic catotelm of peat compared to the predominantly oxic acrotelm, suggesting that brGDGTs are produced by anaerobic bacteria (Weijers et al., 2004, 2006a, 2011), potentially members of the phylum *Acidobacteria* (Weijers et al., 2009; Sinninghe Damsté et al., 2011, 2014). Although the exact source organism(s) are/is currently unknown, in mineral soils (and potentially lakes) the distribution of bacterial brGDGTs is correlated with mean annual air temperature (MAAT) and pH (Weijers et al., 2007; Peterse et al., 2012; De Jonge et al., 2014; Loomis et al., 2014; Li et al.,

2016). Over the past decade ancient deposits of mineral soils (e.g., Peterse et al., 2014) and peat (e.g., Ballantyne et al., 2010) have been used to reconstruct past terrestrial temperatures.

Mineral soils differ from peat as the latter are normally water saturated, consist predominantly of (partially decomposed) organic matter (the organic carbon content of peat is typically >30 wt.%), are typically acidic (pH 3–6), and have much lower density. The combination of these factors means that peat becomes anoxic at relatively shallow depths, whereas mineral soils are typically oxic. Indeed, Loomis et al. (2011) showed that the brGDGT distribution in waterlogged soils is different from that in dry soils and Dang et al. (2016) recently provided direct evidence of moisture control on brGDGT distributions in soils. These differences suggest that microbial lipids in peat might not reflect environmental variables, i.e. pH and temperature, in the same way as they do in mineral soils.

Despite the high concentration of GDGTs in peats relatively few studies have examined the environmental controls on their distribution in such settings (Huguet et al., 2010, 2013; Weijers et al., 2011; Zheng et al., 2015). Those studies found that the application of soil-based proxies to peats can result in unrealistically high temperature and pH estimates compared to the instrumental record. However, owing to the small number of peats that have been studied to date as well as the lack of peatland diversity sampled (the majority of peats sampled for these studies come from temperate climates in Western Europe), the correlation of temperature and pH with brGDGT distribution in peats is poorly constrained. Notably, the lack of tropical peat brGDGT studies limits interpretations of brGDGT distributions in lignite deposits from past greenhouse climates (Weijers et al., 2011).

Here we compare brGDGT distributions in a newly generated global data set of peat with MAAT and (where available) in situ peat pH measurements. Our aim is to gain an understanding of the impact of these environmental factors on the distribution of brGDGTs in peat and develop for the first time peat-specific temperature and pH proxies that can be used to reconstruct past terrestrial climate.

2. MATERIAL AND METHODS

2.1. Peat material

We generated a collection of peat comprising a diverse range of samples from around the world. In total, our database consists of 470 samples from 96 different peatlands. In order to assess the variation in brGDGT distribution within one location, where possible we determined the brGDGT distribution in multiple horizons from within the top 1 m of peat (typically representing several centuries of accumulation) and/or analyzed samples taken at slightly different places within the same peatland. A peat deposit typically consists of an acrotelm and catotelm, although marked heterogeneity can exist even over short distances (Baird et al., 2016). The acrotelm is located above the water table
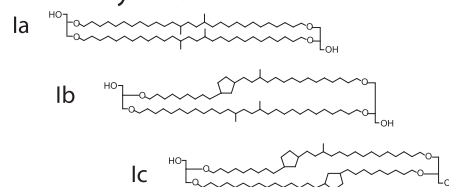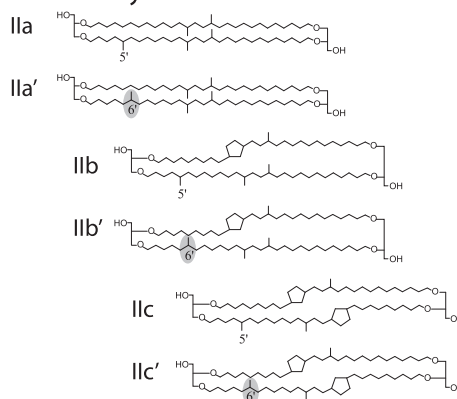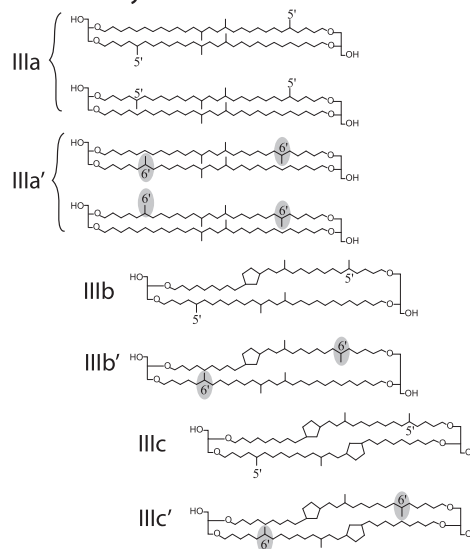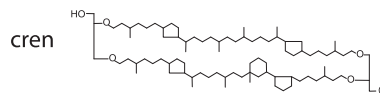
Fig. 1. Structures of brGDGTs (with numbering) as well as isoprenoidal GDGT crenarchaeol (cren), following (De Jonge et al., 2014). Roman numbers indicate tetra- (I), penta- (II), and hexamethylated (III) brGDGTs, whereas letters indicate the absence (a), presence of one (b), or two (c) cyclopentane rings. Prime symbols indicate 6-methyl brGDGTs in which the additional methyl groups of the penta- and hexamethylated brGDGTs occur at the α and/or ω-6 position instead of α and/or ω-5 position of 5-methyl brGDGTs.

for most of the year and characterized by oxic conditions and active decomposition. The acrotelm overlies the cato-telm, which is permanently waterlogged and characterized by anoxic conditions and very slow decomposition. Our dataset spans those biogeochemical gradients (e.g. acro/ca-totelm). Variations in peat accumulation rates differ between sites, implying that the ages of the brGDGT-pool might differ.

Our database includes peats from six continents and all major climate zones, ranging from high latitude peats in Siberia, Canada, and Scandinavia to tropical peats in Indonesia, Africa, and Peru (Fig. 2). It covers a broad range in MAAT from −8 to 27 °C. Although most samples come from acidic peats with pH < 6, the dataset includes several alkaline peats and overall our dataset spans a pH range from 3 to 8. All samples come from freshwater peatlands, except for the one from the Shark River peat (Everglades, USA) that is marine influenced. Unsurprisingly, given their global distribution, the peats are characterized by a wide variety of vegetation, ranging from *Sphagnum*-dominated ombrotrophic peats that are abundant in high-latitude and temperate climates to (sub)tropical peats dominated by vegetation such as *Sagittaria* (arrowhead) and *Cyper-aceae* (sedge), and forested tropical peatlands.

2.2. Environmental parameters

The distribution of brGDGTs was compared to MAAT and *in situ* pH. MAAT was obtained using the simple bio-climatic model PeatStash, which provides surface air tem-peratures globally with a 0.5 degree spatial resolution (for details, see Kaplan et al., 2003; Gallego-Sala and Prentice, 2013). The temperature data in PeatStash is obtained by interpolating long-term mean weather station climatology (temperature, precipitation and the fraction of possible sunshine hours) from around the world for the period 1931–1960 (Climate 2.2 data are available online http://www.pik-potsdam.de/~cramer/climate.html). Cru-cially, mean annual temperatures in peat are similar to MAAT, assuming that the peat is not snow-covered for long periods of time (McKenzie et al., 2007; Weijers

et al., 2011). The temperature at the top surface of (high-latitude) peat can differ from the MAAT due to insolation by snow during winter and intense heating during summer. Despite this, the seasonal temperature fluctuations in peat are dampened at depth as temperatures converge to MAAT (Hillel, 1982; Laiho, 2006; McKenzie et al., 2007; Weijers et al., 2011). We assume that all peat horizons experienced MAAT (the only data available on a global basis). This is likely an oversimplification that introduces some additional uncertainty in our calibration.

Where available, pH data were obtained from measured values reported in the literature or our measurements dur-ing sampling. For peats, pH cannot be determined using dried material, as is normally done for soils (Stanek, 1973). Accurate pH measurements can only be obtained from *in situ* measurements, especially for groundwater-fed wetlands, and these are not available for all locations.

2.3. Lipid extraction

For the majority of samples (>430 out of 470), between 0.1 and 0.5 g of dried bulk peat were extracted with an Ethos Ex microwave extraction system with 20 mL of a mixture of dichloromethane (DCM) and methanol (MeOH) (9:1, v/v) at the Organic Geochemistry Unit (OGU) in Bris-tol. The microwave program consisted of a 10 min ramp to 70 °C (1000 W), 10 min hold at 70 °C (1000 W), and 20 min cool down. Samples were centrifuged at 1700 rounds per minute for 3 to 5 min and the supernatant was removed and collected. 10 mL of DCM:MeOH (9:1) were added to the remaining peat material and centrifuged again after which the supernatant was removed and combined with the previously obtained supernatant. This process was repeated 3 to 6 times, depending on the amount of extracted material, to ensure that all extractable lipids were retrieved. The total lipid extract (TLE) was then concentrated using rota-evaporation. An aliquot of the TLE (typically 25%) was washed through a short (<2 cm) silica column using DCM:MeOH (9:1) to remove any remaining peat particles. The TLE was dried under a gentle nitrogen flow and then
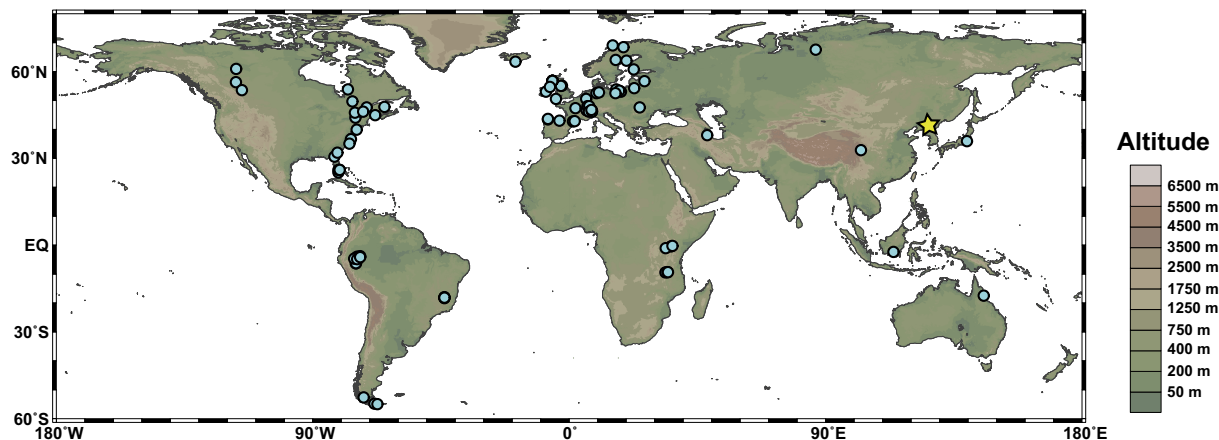

Fig. 2. Map with the location of all peats used in this study. The star indicates the location of the Hani peat sequence in NE China.

re-dissolved in hexane/*iso*-propanol (99:1, v/v) and filtered using 0.45 μm PTFE filters.

A small number of peats were extracted using different methods and either the TLE or polar fraction was analyzed for GDGTs (see Table S1). Samples from the Kyambangunguru peat in Tanzania were extracted using the Bligh–Dyer protocol. Previous work on peat demonstrated that the brGDGT distribution is similar using Bligh–Dyer extraction as Soxhlet extraction (Chaves Torres and Pancost, 2016). The TLE was cleaned over a short Si column at the OGU in Bristol. Both cleaned TLE and polar fractions were re-dissolved in hexane/*iso*-propanol (99:1, v/v) and filtered using 0.45 μm PTFE filters.

2.4. Analytical methods

All samples were analyzed for their core lipid GDGT distribution by high performance liquid chromatography/ atmospheric pressure chemical ionisation – mass spectrometry (HPLC/APCI-MS) using a ThermoFisher Scientific Accela Quantum Access triplequadrupole MS. Normal phase separation was achieved using two ultra-high performance liquid chromatography silica columns, following Hopmans et al. (2016). Crucially this method allows for the separation of the 5- and 6-methyl brGDGT isomers. Injection volume was 15 μL, typically from 100 μL. Analyses were performed using selective ion monitoring mode

(SIM) to increase sensitivity and reproducibility (*m/z* 1302, 1300, 1298, 1296, 1294, 1292, 1050, 1048, 1046, 1036, 1034, 1032, 1022, 1020, 1018, 744, and 653). The results were integrated manually using the Xcalibur software. Based on daily measurements of an in–house generated peat standard, analytical precession (σ) over the 12 months during which the data were analyzed is 0.01 for the proxy index we define below (MBT$'_{5me}$, Eq. (2)).

2.5. Proxy calculation

Guided by previous studies we used a range of proxies to express ratios of different GDGTs and the nomenclature of De Jonge et al. (2014) (Fig. 1).

$$MBT = \frac{(Ia + Ib + Ic)}{(Ia + Ib + Ic + IIa + IIa' + IIb + IIb' + IIc + IIc' + IIIa + IIIa' + IIIb + IIIb' + IIIc + IIIc')} \quad (1)$$

The original methylation of branched tetraether (MBT) index compared the relative abundance of tetramethylated brGDGTs (compounds Ia–Ic) to that of penta- (compounds IIa–IIc') and hexamethylated (compounds IIIa–

IIIc') brGDGTs that have one or two additional methyl groups (Weijers et al., 2007). It was recently discovered that the additional methyl groups in penta- and hexamethylated brGDGTs can also occur at the C6 position (6-methyl brGDGTs, indicated by a prime symbol; e.g. brGDGT-IIa'): the 6-methyl penta- and hexamethylated brGDGTs (De Jonge et al., 2013). Excluding the 6-methyl brGDGTs from the MBT index resulted in the MBT$'_{5me}$ index. In the global soil database the application of MBT$'_{5me}$ led to an improved correlation with temperature (De Jonge et al., 2014).

$$MBT'_{5ME} = \frac{(Ia + Ib + Ic)}{(Ia + Ib + Ic + IIa + IIb + IIc + IIIa)} \quad (2)$$

In addition to different number of methyl groups, brGDGTs can contain up to two cyclopentane moieties (e.g., brGDGT-Ib and -Ic). CBT' is a modified version of the original cyclisation of branched tetraether (CBT) index (Weijers et al., 2007) and in soils CBT' has the best correlation with pH (De Jonge et al., 2014):

$$CBT' = \log\left(\frac{Ic + IIa' + IIb' + IIc' + IIIa' + IIIb' + IIIc'}{Ia + IIa + IIIa}\right) \quad (3)$$

The isomer ratio of 6-methyl brGDGTs (IR$_{6me}$) reflects the ratio between 5- and 6-methyl brGDGTs (Yang et al., 2015) with low (high) values indicative of a dominance of 5-methyl (6-methyl) brGDGTs:

$$IR_{6me} = \left(\frac{IIa' + IIb' + IIc' + IIIa' + IIIb' + IIIc'}{IIa + IIa' + IIb + IIb' + IIc + IIc' + IIIa + IIIa' + IIIb + IIIb' + IIIc + IIIc'}\right) \quad (4)$$

The isomerization of branched tetraethers (IBT) is related to IR$_{6me}$ but reflects the isomerization of brGDGT-IIa and -IIIa only (Ding et al., 2015):

$$IBT = -\log\left(\frac{IIa' + IIIa'}{IIa + IIIa}\right) \quad (5)$$

The branched versus isoprenoidal tetraether (BIT) index (Hopmans et al., 2004) reflects the relative abundance of the major bacterial brGDGTs versus a specific archaeal isoGDGT, crenarchaeol (Fig. 1), produced by *Thaumarchaeota* (Sinninghe Damsté et al., 2002):

$$BIT = \frac{Ia + IIa + IIa' + IIIa + IIIa'}{Ia + IIa + IIa' + IIIa + IIIa' + cren.} \quad (6)$$

Finally, the isoprenoidal over branched GDGT ratio ($R_{i/b}$), related to the BIT index, records the relative abundance of archaeal isoGDGTs over bacterial brGDGTs (Xie et al., 2012).

$$R_{i/b} = \frac{\sum isoGDGTs}{\sum brGDGTs} \qquad (7)$$

2.6. Statistical methods

Temperature and pH calibrations were obtained using the average proxy value for each peat and Deming regressions. The software we used was RStudio (R Studio Team, 2015) and Method Comparison Regression (MCR) package (Manuilova et al., 2014), which are freely available to download[1]. The Rscript and data are available in the appendices.

Deming regressions differ from simple linear regression, which so far have been used in brGDGT proxy calibrations, as they account for error in the data on both the x- (e.g., proxy) and y-axis (e.g., environmental variable) (Adcock, 1878).

We used the average proxy value for each peat to calculate Deming regressions, calibration errors (RMSE, see below), and calibration coefficients of determination (R^2). The errors associated with proxy measurements (e.g. MBT'_{5me}) and environmental parameters (MAAT/pH) are independent and assumed to be normally distributed. To calculate a Deming regression, the ratio of variances (δ) must be calculated. For MAAT we took a standard deviation (σ) of 1.5 °C based on the estimated mean predictive error of up to 1.4 °C for mean temperature in a similar dataset (New et al., 1999). For pH we took a standard deviation of 0.5 based on the average reported heterogeneity in pH for the peatlands used in the database (see Supplementary Table 1). For MBT'_{5me}, CBT', and CBT_{peat} we calculated the average standard deviation of each proxy from the entire peat data set (0.05, 0.25, and 0.2, respectively). This results in a ratio of variances of 0.0011 for the MBT'_{5me}/MAAT calibration and 0.25 and 0.16 for the pH calibration based on CBT' and CBT_{peat}, respectively. Residuals were calculated for the full dataset and using

$$Residual_y = y_{observed} - y_{predicted} \qquad (8)$$

The root mean square error (RMSE) for y, the predictive error for the environmental parameter of interest (MAAT or pH), was calculated for the average proxy value of each peat and using

$$RSME_y = \sqrt{\frac{\sum_{x=1}^{n}(y_{x,observed} - y_{x,predicted})^2}{n} \times \frac{n}{df}} \qquad (9)$$

Where df stands for degrees of freedom, which in this case is n-1.

3. RESULTS

Although we did not calculate concentrations, based on changes in signal intensity the relative abundance of GDGTs was always higher at depth compared to the top ($\sim$0–20) cm of peat. BIT indices (Eq. (6)) range between 0.75 and 1, but 99% of the samples have a BIT

value $\geqslant 0.95$. Similarly, $R_{i/b}$ ratios are typically <0.5. Only three samples from the São João da Chapada peat in Brazil have a $R_{i/b}$ ratio >1.

The majority of brGDGTs are tetramethylated and 5-methyl penta- and hexamethylated brGDGTs. The most abundant brGDGTs in peat are brGDGT-Ia and IIa. By extension, the IR_{6me} ratio (Eq. (4)) is low. brGDGTs containing cyclopentane moieties are much less abundant than acyclic brGDGTs and brGDGT-IIIb(') and -IIIc(') are either below detection limit or present at trace abundances ($\leqslant$1% of total brGDGTs). Indeed, three brGDGTs dominate the entire global dataset: tropical peats contain almost exclusively brGDGT-Ia (up to 99% of total brGDGTs), whereas in high-latitude peats brGDGT-IIa and -IIIa are dominant (Fig. 3).

4. DISCUSSION

The observation that $R_{i/b}$ ratios are low in most peats is consistent with previous observations that bacterial brGDGTs dominate over archaeal isoprenoidal GDGTs in peat (Schouten et al., 2000; Sinninghe Damsté et al., 2000; Pancost et al., 2003) and mineral soils (Hopmans et al., 2004).

4.1. Shallow vs deep GDGT distributions

The apparent increase in GDGT abundance with depth is consistent with previous observations in peatlands (Weijers et al., 2004; Peterse et al., 2011) and reflects the combined effects of preferential GDGT production in anaerobic settings and the accumulation of fossil GDGTs over time at depth (Liu et al., 2010; Weijers et al., 2011).

In one high-latitude peat (Saxnäs Mosse, Sweden) the distribution of both intact polar lipids (compounds still containing a polar head groups) and core brGDGTs (compounds having lost their polar head group) differed between the acro- and catotelm and brGDGT abundances were much higher in the latter (Weijers et al., 2009; Peterse et al., 2011). Based on these results Peterse et al. (2011) speculated that microbial communities differed between the oxic acrotelm and anoxic catotelm. As oxygen content can influence cellular lipid composition of bacteria, Huguet et al. (2010) speculated that oxygen availability could be one of the factors directly influencing the brGDGT synthesis by bacteria in peat, as opposed to influencing the type of source organism(s). Studies from lakes also suggested that changes in lake oxygenation state can influence the brGDGT distribution (Tierney et al., 2012; Loomis et al., 2014).

Our dataset consists of a mixture of surface (0–15 cm) and deeper samples that extend through the top one meter of peat. For the majority of peats there is no detailed information available on water table depths and location of the acro/catotelm boundary. Nonetheless, to provide a first order assessment on whether there is a systematic and significant difference in core brGDGT distribution between the upper (assumed to be generally oxic) and underlying anoxic peat, we compared the relative abundance of the three most abundant brGDGTs (Ia, IIa, and IIIa) in the
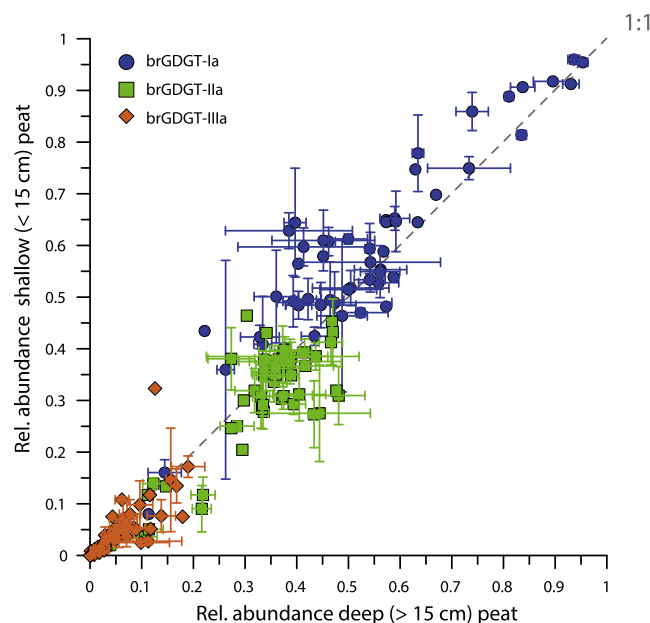

Fig. 3. Fractional abundances of the three main brGDGTs in the top 15 cm of each peat (assumed to be representative of the oxic acrotelm) versus the fractional abundance of these brGDGTs between 15 and 100 cm in the peat (assumed to be representative for the anoxic catotelm). For peats where multiple samples were analyzed, error bars represent 1σ from the average fractional abundance.

shallow surface peat (top 15 cm) with that of the deep peat below 15 cm (Fig. 3), although we acknowledge that this is likely an oversimplification.

There are some differences. In general the relative abundance of brGDGT-Ia is slightly higher in the top 15 cm of a peat compared to the peat below 15 cm, especially when its abundance is <60%. Overall, however, the distributions plot along the 1:1 line, indicating that there is no systematic difference in brGDGT distribution between the (assumed) oxic surface and the peat below 15 cm (likely anoxic). This does not preclude differences in brGDGT production between oxic and anoxic conditions, but this appears to be primarily expressed via greater production of brGDGTs under anoxic conditions as demonstrated by the higher abundance of GDGTs across the acro/catotelm boundary (Weijers et al., 2006a). These results provide indirect evidence that oxygen availability does not significantly impact the degree of methylation of (core) brGDGTs. One possible explanation for why oxygen availability does not affect distributions is that brGDGTs could be predominantly produced by anaerobes throughout the peat, in low abundance in anaerobic microenvironments in shallow peat and in high abundance in the anaerobic catotelm.

Several (high-latitude) peats, however, do appear to exhibit strong variations between deep and shallow sections of the peat. The down core records from Stordalen (Sweden) and Andorra (S. Patagonia), for example, are characterized by a large and abrupt shift in brGDGT distribution at depth (Fig. 4). The MBT$'_{5me}$ indices recorded at the very top of these high-latitude peats are between 0.8 and 0.6, as high as those found in mid-latitude and subtropical peats, but decrease to values between 0.2 and 0.4 below ∼30 cm. Peats from temperate climates (e.g. Walton moss, UK) and the tropics (e.g. Sebangau, Indonesia) display much

smaller or no change in brGDGT distribution with depth (Figs. 4 and 5). It appears that this offset in brGDGT distribution with depth is amplified in high-latitude peats. This is consistent with previous studies that indicated a difference in brGDGT-distribution between the acro- and catotelm in a high-latitude peat from southern Sweden (Weijers et al., 2009; Peterse et al., 2011).

We argue that the high MBT$'_{5me}$ values at the top of these high-latitude peats are heavily biased towards summer temperatures. At these settings winter temperatures are often below freezing for a prolonged period, likely causing bacterial growth and GDGT production to slow down significantly. Summer temperatures are much higher (e.g. mean warmest month temperature at Stordalen is around 13 °C), in-line with the observed relatively high MBT$'_{5me}$ values (e.g., 0.6–0.7 at Stordalen, see Fig. 4). Deeper in the peat, seasonal temperature fluctuations are much less pronounced and temperatures rapidly converge to the MAAT (Vitt et al., 1995; Laiho, 2006; McKenzie et al., 2007; Weijers et al., 2011), likely accounting for the lower MBT$'_{5me}$ values in the deeper peat horizons. Moreover, the greater production of GDGTs in the anaerobic part of the peat will cause GDGT-based temperatures to rapidly converge on the deep peat growth temperature, overprinting the seasonal summer bias of fossil GDGTs synthesized at the surface.

This effect is diminished in temperate and especially tropical peatlands from around sea level, which we attribute to the lack of a preferred growing season in settings with smaller seasonal temperature ranges. In such settings temperatures are less frequently (or never) below freezing and brGDGT production in the top of the peat likely occurs for all or most of the year, such that GDGTs produced in both the shallow and deeper part of the peat record MAAT.
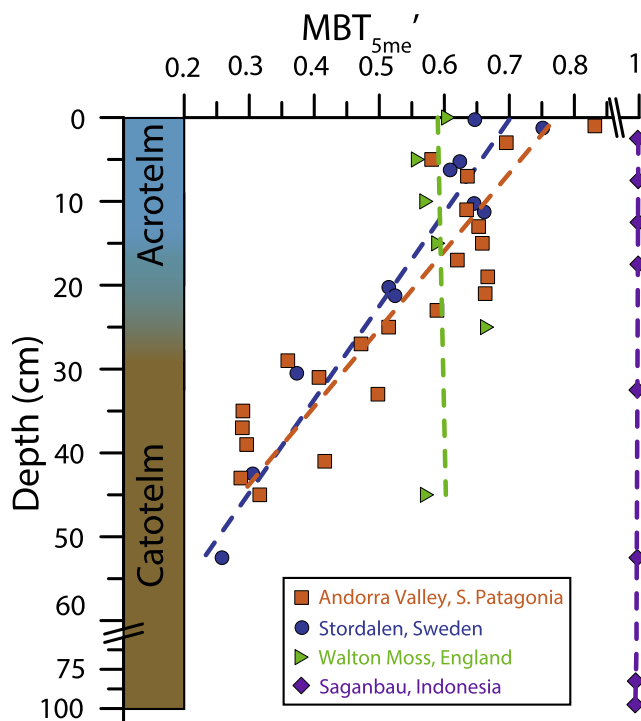
Fig. 4. Down core record of MBT'_{5me} in four peats a high-latitude peat from Sweden (blue squares), high-latitude peat from Patagonia (orange squares), temperate peat from the UK (green triangles), and tropical peat from Indonesia (purple diamonds). (For interpretation of the references to color in this figure legend, the reader is referred to the web version of this article.)
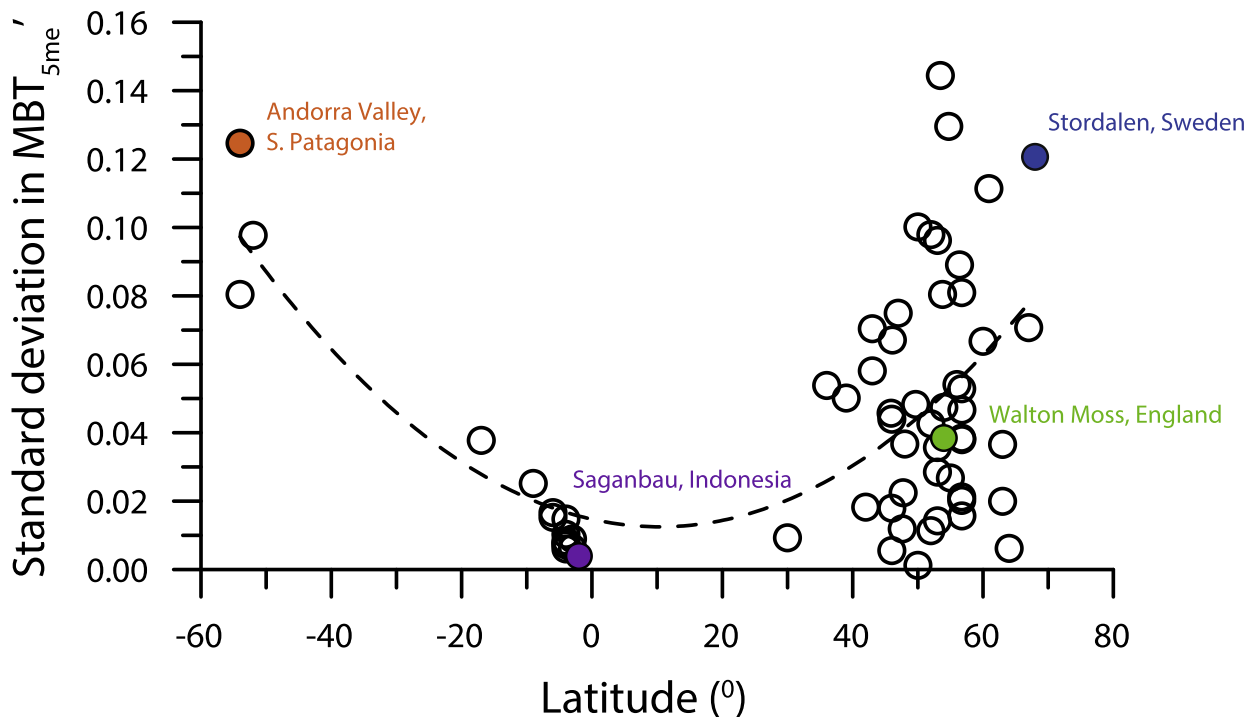

Fig. 5. Standard deviation of MBT'_{5me} for each low-altitude (<1000 m) peat versus latitude. The four peats used in Fig. 4 are highlighted.

This hypothesis needs further testing but indicates that (1) brGDGT production may be biased towards the warm season in the upper part of high-latitude/altitude peats; (2)

care has to be taken when interpreting brGDGT-based trends in the top of such peats; and (3) the temperature signal in such peats is imparted at depth, such that downcore

GDGT variations in ancient peat archives could potentially be temporally offset (precede) the climate events that caused them. However, as brGDGTs in long peat cores, and by extension ancient lignites (fossilized peats), are dominated by production at depth where temperature equals MAAT (see Section 2.2) it is very unlikely that temperatures obtained from these archives are seasonally biased.

In the remainder of this work, for high-latitude peats that show a clear offset between the top and deeper part of the peat we use only the average GDGT distribution from below 20 cm, as the majority of change appears to occur in the top 20 cm. For the other peats we retain all data from the upper 1 m, not differentiating between the acro- and catotelm. To generate the temperature and pH calibrations we use the average brGDGT distribution for each peatland. For peats where multiple samples were analyzed, error bars indicate the deviation (1σ) from the average.

4.2. Influence of temperature and pH on brGDGTs in peats

It is well established that in soils and lakes, environmental conditions such as temperature and pH are highly correlated with the brGDGT distribution (e.g.,Weijers et al., 2007; Peterse et al., 2012; Schoon et al., 2013; De Jonge et al., 2014; Loomis et al., 2014; Xiao et al., 2015; Li et al., 2016). In the following sections we investigate the influence of these parameters on the brGDGT distribution in peat using the average proxy value (e.g. MBT'_{5me}) for each peatland.

4.2.1. Influence of peat pH on brGDGT distribution

Weijers et al. (2007) demonstrated that in a global mineral soil database the degree of cyclisation of brGDGTs is correlated to pH, with a higher fractional abundance of brGDGTs that contain cyclopentane moieties in soils with a higher pH. Following the discovery of 6-methyl brGDGTs (De Jonge et al., 2013), it was shown that the degree of isomerization of brGDGTs, the ratio of 6-methyl versus 5-methyl brGDGTs, is also correlated to soil pH, with a higher fractional abundance of 6-methyl brGDGTs in soils with a higher pH (De Jonge et al., 2014; Xiao et al., 2015). Owing to the limited pH range of the few peats used to study brGDGTs so far and because all of these studies pre-date the recent analytical advances that allow for the separation of 5- and 6-methyl brGDGTs, it is unknown whether pH has an influence on brGDGTs in peats or whether the dependence is similar to that found in soils. Our peat database spans a pH range from 3 to 8, similar to that of the soil database, allowing us to assess the influence of pH on the brGDGT distribution in such settings.

Although pH measurements are only available in 51 out of 96 peats, our results indicate that 6-methyl brGDGTs are present at either only trace abundances ($\text{IR}_{6me} < 0.1$) or are absent in acidic peats with pH < 5.4 (Fig 6). Higher ratios occur in peats with higher pH. The highest ratio (0.58) occurs in the marine-influenced alkaline peat from the Everglades. Not surprisingly, the fractional abundances of the three most common 6-methyl brGDGTs (brGDGT-IIa′, -IIb′, -IIIa′) are significantly correlated with pH with R-values between 0.4 and 0.6 ($p < 0.01$) (Fig. 7). These results are consistent
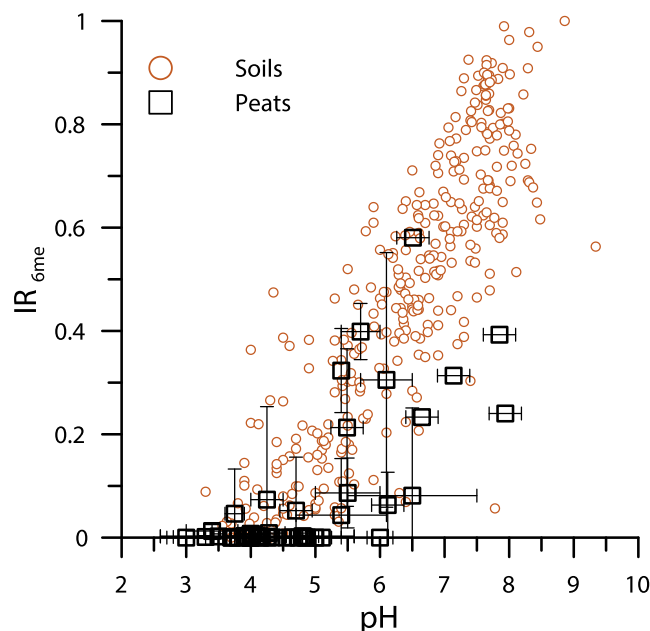

Fig. 6. Ratio of 6-methyl over 5-methyl brGDGTs (IR_{6me}) versus pH for peat samples (black squares) together with the IR_{6me} in the top 10 cm of mineral soils (orange circles) (De Jonge et al., 2014; Ding et al., 2015; Xiao et al., 2015; Yang et al., 2015; Lei et al., 2016). Vertical error bars on the peat data represent 1σ and are based on the analysis of multiple horizons from the same peat. Horizontal error bars represent the spread in pH reported for each peat. (For interpretation of the references to color in this figure legend, the reader is referred to the web version of this article.)
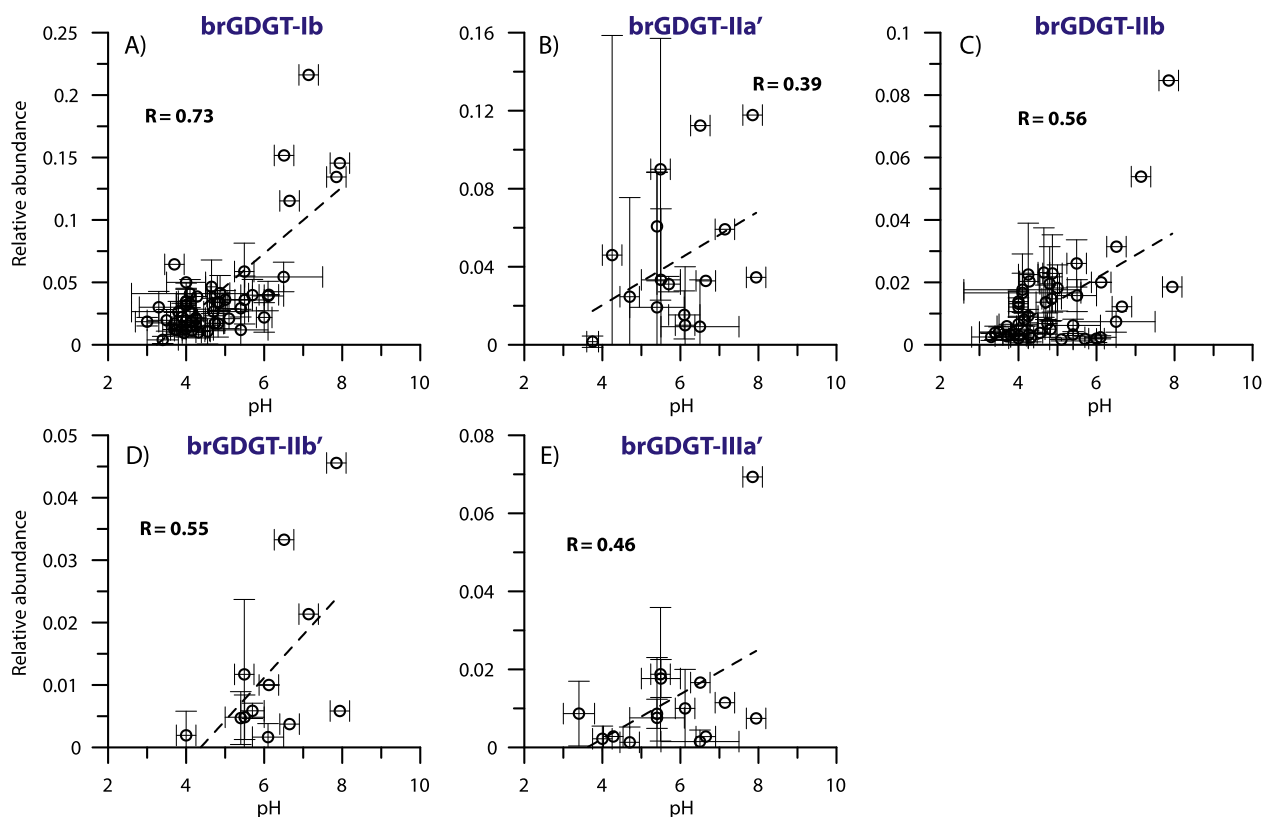
Fig. 7. Fractional abundance of brGDGT versus pH for those compounds with a *r*-value greater than 0.45 (A) brGDGT-Ib, (B) brGDGT-IIa′, (C) brGDGT-IIb, (D) brGDGT-IIb′, and E) brGDGT-IIIa′ ($p < 0.01$ for all compounds). Samples with fractional abundances <0.001 are not included. Vertical error bars represent 1σ and are based on the analysis of multiple horizons from the same peat. Horizontal error bars represent the spread in pH reported for each peat.

with observations from soils that indicate a positive correlation between the fractional abundance of 6-methyl brGDGTs and pH (De Jonge et al., 2014; Xiao et al., 2015).

As a result, the IR$_{6me}$ as well as the related IBT index, both of which have been used to reconstruct pH in soils (Ding et al., 2015; Xiao et al., 2015), are correlated with pH in the peats (not shown). However, this comparison is complicated by the fact that 6-methyl brGDGTs are absent in many of the peats. For IR$_{6me}$ the absence of 6-methyl brGDGTs results in values that are 0, whereas IBT cannot be calculated for samples that lack 6-methyl brGDGTs as the logarithm of zero is undefined.

The abundance of 6-methyl brGDGTs is generally lower in peats than in mineral soils with comparable pH. Indeed, 6-methyl brGDGTs are present in 99% of all soils in the global soil database, including soils with pH < 5 where IR$_{6me}$ ratios can be as high as 0.4 (Fig. 6). Recent work has shown that in addition to pH the fractional abundance of 6-methyl brGDGTs is negatively correlated with soil water content, with fewer 6-methyl brGDGTs versus 5-methyl brGDGTs in soils with 60% water content compared to soils with <10% water content (Dang et al., 2016). It is likely that the negative correlation between soil water content and fractional abundance of 6-methyl brGDGTs can explain the overall lower IR$_{6me}$ in peats as these are generally water saturated.

In addition to 6-methyl brGDGTs, the fractional abundances of brGDGTs containing cyclopentane moieties (brGDGT-Ib and -IIb) are also significantly correlated to pH ($R = 0.73$ and 0.56, $p < 0.01$, respectively) (Fig. 7a and c). The other brGDGTs are not significantly correlated to pH. These observations are consistent with those from soils, where both 5- and 6-methyl brGDGTs containing cyclopentane moieties are more abundant at higher pH (Weijers et al., 2007; Peterse et al., 2012; De Jonge et al., 2014). Consequently, and similar to soils (De Jonge et al., 2014; Xiao et al., 2015), CBT′ (Eq. (3)) in peat can be modeled as a function of pH (Fig. 8):

$$pH = 2.69 \times CBT' + 9.19 (n = 50, \quad R^2$$
$$= 0.44, \quad RMSE = 1.0) \tag{10}$$

The slope of this calibration is different (higher) from that found in soils (see supplementary information), but the coefficient of determination is lower, and the RMSE is higher. A stronger correlation is obtained by using only compounds that are significantly correlated to pH in the numerator, CBT$_{peat}$:

$$CBT_{peat} = \log \left(\frac{Ib + IIa' + IIb + IIb' + IIIa'}{Ia + IIa + IIIa} \right) \tag{11}$$

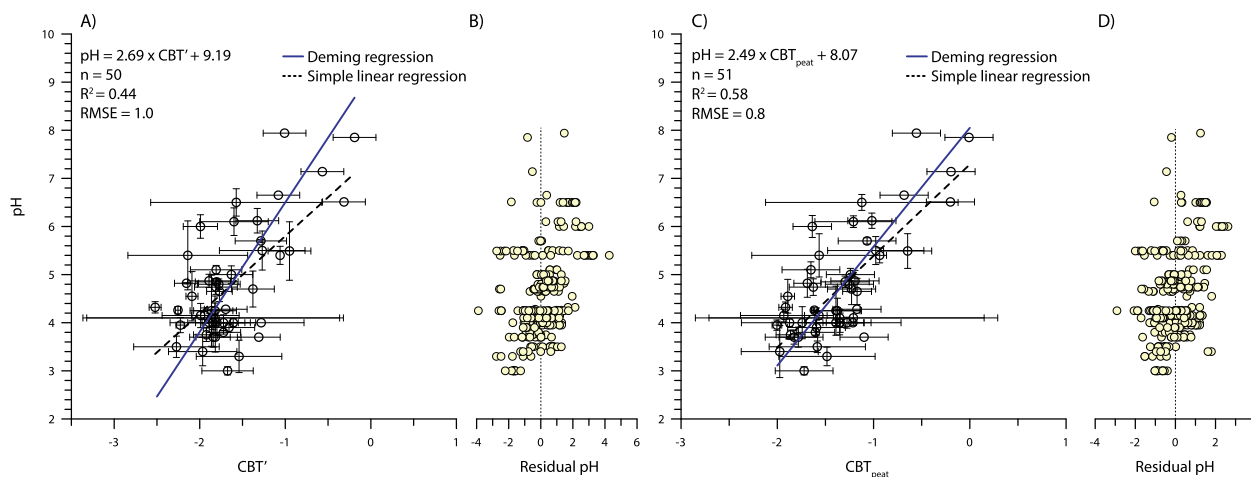$$pH = 2.49 \times CBT_{peat} + 8.07 \quad (n = 51, \quad R^2$$
$$= 0.58, RMSE = 0.8) \tag{12}$$

Fig. 8. (A) Average CBT′ for each peat versus pH (black circles) and (C) average CBT$_{peat}$ for each peat versus pH (black circles). Solid blue lines in A and C represent the Deming regression used to obtain the calibrations, while dashed black lines reflect simple linear regressions. Horizontal error bars represent 1σ and are based on the analysis of horizons samples from the same peat. Vertical error bars represent the spread in pH reported for each peat. Also shown is the residual pH for all analyzed peat samples (yellow circles), obtained by subtracting the estimated pH using the CBT′ (B) and CBT$_{peat}$ (D) deming calibrations from the observed pH. (For interpretation of the references to color in this figure legend, the reader is referred to the web version of this article.)

Although the coefficient of determination increases and RMSE decreases using CBT$_{peat}$, the calibration uncertainties are still larger than those reported for soils (see supplementary information).

It is noteworthy that in peats the correlation between brGDGT distributions and pH is much weaker than that with MAAT (see below). This contrasts with mineral soils, for which the correlation of CBT′ with pH ($R^2 = 0.85$), is stronger than that of MAT$_{mr}$ with MAAT ($R^2 = 0.68$) (De Jonge et al., 2014). The weaker correlation can partly be explained by the smaller sample set used for the peat calibration ($n = 51$) versus soil calibration ($n = 221$). However, taking 51 random mineral soils from the latter still yields a stronger correlation between CBT′ and pH than we obtain for the peat data set. In addition, the coefficient of determination of a calibration based only on peats with pH ⩾ 5 is ∼0.5 for CBT$_{peat}$, similar to that of the complete data set. We argue that the difference could be related to the observation that in mineral soils water content also influences the brGDGT distribution, especially that of 6-methyl brGDGTs (e.g., Menges et al., 2014). Recently Dang et al. (2016) showed that CBT$_{(5me)}$ is higher in dry soils compared to wet soils. Because alkaline soils are often also dry whereas acidic soils are often wet, this effect could enhance the correlation between CBT′ and pH in soils. As peats are typically water saturated, the additional effect of soil water content is lacking, which may explain the weaker correlation between CBT′ and pH in peats compared to mineral soils.

4.2.2. Influence of MAAT on brGDGTs in peats

In mineral soils the distribution of brGDGTs is influenced by MAAT, with the degree of methylation decreasing as temperature increases (Weijers et al., 2007; De Jonge et al., 2014). A temperature effect on the brGDGT distribution was recently also found in one peatland (Huguet et al., 2013). Although the producers of brGDGTs are currently

unknown, such a response is consistent with homeoviscous adaptation (Weijers et al., 2007). Here we investigate whether temperature has a significant correlation with brGDGTs in peats on a global scale.

When plotted against MAAT, only 5-methyl brGDGTs lacking cyclopentane moieties (brGDGT-Ia, -IIa, and -IIIa) have significant correlations with MAAT (Fig. 9). brGDGT-Ia is positively correlated with MAAT ($R = 0.72$, $p < 0.01$), whereas brGDGT-IIa ($R = 0.82$, $p < 0.01$), and -IIIa ($R = 0.63$, $p < 0.01$) are negatively correlated with MAAT. These correlations are significantly higher than those found in the global soil data set (De Jonge et al., 2014). The degree of methylation of 5-methyl brGDGTs is captured in the MBT′$_{5me}$ index (Eq. (2)). As such we use the MBT′$_{5me}$ index to construct a peat-specific temperature proxy (Fig. 10):

$$MAAT_{peat} \ (^{\circ}C) = 52.18 \times MBT'_{5me} - 23.05$$
$$(n = 96, \ R^2 = 0.76, \ RMSE = 4.7) \quad (13)$$

Crucially, no correlation is observed between MBT′$_{5me}$ and pH ($R^2 = 0$ and $p > 0.8$) and we observe no trend in the residuals. The coefficient of determination (R^2) of MAAT$_{peat}$ is higher compared to a Deming regression of the expanded soil dataset ($R^2 = 0.60$, see supplementary information) as well as that of the linear MBT′$_{5me}$ calibration ($R^2 = 0.66$) suggested by De Jonge et al. (2014). Crucially, because the slope of the MAAT$_{peat}$ calibration is steeper, it could have greater utility for the reconstruction of tropical temperatures (MAAT$_{peat}$ reaches saturation at 29.1 °C), although these maximum temperatures are higher than the maximum MAAT in the modern calibration data set which is 26.7 °C. In contrast, the Deming MBT′$_{5me}$ soil calibration reaches saturation (i.e. MBT′$_{5me}$ = 1) at a temperature of 24.8 °C (see supplementary information), while the linear MBT′$_{5me}$ calibration suggested by De Jonge et al. (2014) has a maximum of 22.9 °C.
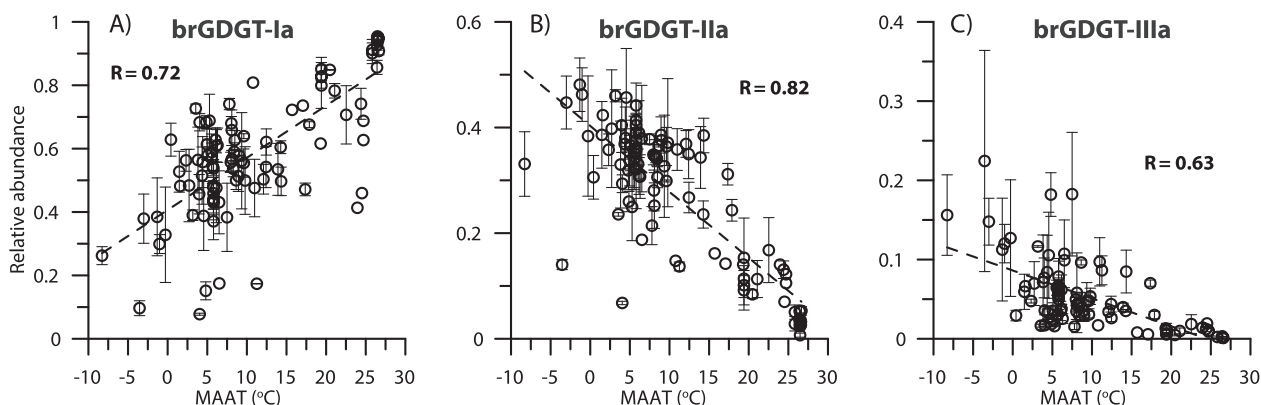
Fig. 9. Fractional abundance of the three main brGDGT versus MAAT (A) brGDGT-Ia, (B) brGDGT-IIa, and (C) brGDGT-IIIa ($p < 0.01$ for all compounds). Samples with fractional abundances <0.001 were not included. Vertical error bars represent 1σ and are based on the analysis of multiple horizons from the same peat.
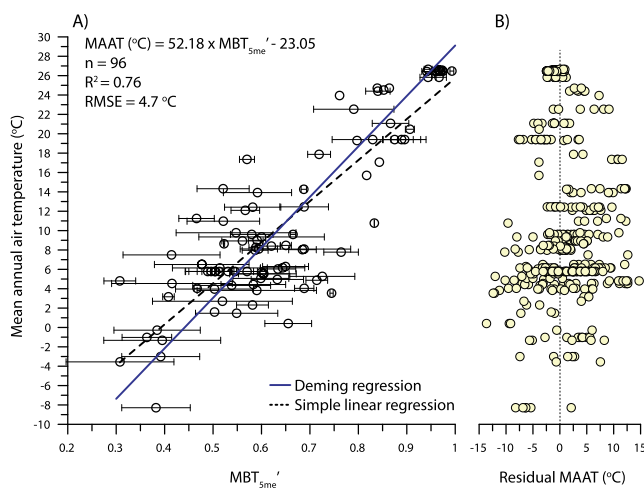

Fig. 10. Average MBT'_{5me} for each peat versus MAAT (black circles). The solid blue line represents the Deming regression, whereas dashed lines reflect the simple linear regression. Horizontal error bars represent 1σ and are based on the analysis of multiple horizons from the same peat. Also shown is the residual MAAT of all analyzed peat samples (yellow circles) obtained by subtracting the estimated MAAT using the MBT'_{5me} Deming calibration from the observed MAAT. (For interpretation of the references to color in this figure legend, the reader is referred to the web version of this article).

4.3. Implications for paleoclimate reconstructions and future work

Compared to the natural archives previously used to reconstruct past terrestrial temperature change (e.g., riverine, lacustrine, and marine sediments), peats have a major advantage. For example, the brGDGTs in peat are mainly derived from *in situ* production. Mixing of brGDGT source areas, which complicates the application of GDGTs in sediments that represent a large catchment area (e.g., Zell et al., 2014; De Jonge et al., 2015; Sinninghe Damsté, 2016), is unlikely to be a problem. In addition, peats are overall characterized by anoxic conditions and the preservation potential of organic compounds such as brGDGTs is high. Finally, as peats are water saturated, especially the catotelm where the majority of brGDGT production occurs, the additional influence of changes in moisture content (Menges et al., 2014; Dang et al., 2016) is also negligi-

ble. Nevertheless, there are limitations to this proxy that need to be considered when evaluating suitable palaeoclimate applications, and we explore those below.

4.3.1. Late Holocene climate

Here we provide peat-specific temperature and pH proxies that could be used to reconstruct terrestrial climate over a broad range of time scales, including the late Holocene. However, the estimated variation in terrestrial temperature of most places on earth during the last millennium is typically less than 1 °C (Mann et al., 2009; Pages 2k Consortium, 2013), although there could be local exceptions. Such temperature change is much smaller than the calibration error (RMSE of ~4.7 °C). Although based on different lipids produced by different organisms, GDGT proxies can potentially record temperature changes smaller than the calibration errors when utilized within a highly constrained site-specific study (Tierney et al., 2010), although

this interpretation was recently contested (Kraemer et al., 2015).

Regardless of calibration issues, application of the MAAT$_{peat}$ calibration to late Holocene palaeoclimate remains problematic. A potential seasonal bias in the top of some high-latitude peats, as well as a potential difference between oxic and anoxic production, appear to prevent application of this proxy to shallow peat sediments. Indeed, our downcore profiles spanning the top 1 meter of peat exhibit changes in brGDGT distributions equivalent to temperature variations of up to several degrees Celsius, larger than the expected climate variations. Moreover, as discussed above, GDGTs appear to be predominantly generated at depth, and although this evidently ensures they record MAAT it does mean that their reconstructed temperature signals start in deeper peat horizons, i.e. stratigraphically preceding the climate changes that caused them.

Future work should determine whether these peat-specific proxies can be used to reconstruct small amplitude and/or short-lived temperature variation. However we currently urge caution in applying the peat-specific proxies to shallow peat cores to reconstruct late Holocene climate (e.g., Little Ice Age or Medieval Warm anomaly).

4.3.2. Application to the last glacial

We envision these proxies are well-suited to reconstruct large amplitude and more long-term temperature excursions such as those associated with the last glacial termination and early Holocene. Such transitions are recorded in some particularly long peat cores at several places around the world (e.g., McGlone et al., 2010; Vanneste et al., 2015; Zheng et al., 2015; Baker et al., 2016). To test whether the novel peat-specific temperature calibration can be used to reconstruct glacial/interglacial temperature variability, we applied this proxy to samples from the Hani peat sequence (Fig. 2). Hani peat is located in northeastern China and in places is up to 10 meters thick, spanning ~16,000 cal yrs (Zhou et al., 2010). We analyzed two samples from ~840 cm depth (corresponding to the late glacial at around 15.3 kyr), and compared MAAT$_{peat}$ with that of two samples from around 100 cm depth (corresponding to the late Holocene with an age of 700–1000 yrs). Using MAAT$_{peat}$ we obtained an average temperature of around −0.8 °C for the late glacial (15.3 kyr). For the late Holocene (0.7–1 kyr) we obtained an average temperature of around 4.6 °C (Table 1).

Taking the calibration error of ~4.7 °C into account the reconstructed late Holocene temperatures (4.6 °C) are close to the observed modern-day MAAT of around 4 °C at this locality (Zhou et al., 2010). In contrast, applying soil cali-

brations to reconstruct MAAT at this site results in significantly higher values (up to 11 °C; Table 1). MAAT$_{peat}$ (as well as the soil MBT$'_{5me}$ calibration) indicates that temperatures increased from the late glacial to the late Holocene by around 5 °C. In contrast the MAT$_{mr}$ mineral soil calibration indicates a smaller increase of around 3 °C. A ~5 °C increase is similar to that observed in east Asian loess-paleosol sequences (Peterse et al., 2014), although that is based on the MBT($'$)/CBT method. In addition a 5 °C deglacial temperature increase is similar to those of several sea surface temperature records available from similar latitudes in the Sea of Japan (Lee, 2007). The next step should be multiproxy temperature reconstructions in a variety of locations to test the new calibration and to determine whether absolute temperatures obtained using MAAT$_{peat}$ are reliable. Nonetheless, this initial analysis indicates that MAAT$_{peat}$ yields temperature estimates that are consistent with both modern day observations and other proxy estimates for the last glacial.

4.3.3. Deep time application

We see considerable scope for future work with this proxy to reconstruct terrestrial temperature during past greenhouse periods and across hyperthermals (e.g. Paleocene/Eocene Thermal Maximum; PETM). These events are recorded in lignite deposits. For example the PETM is documented in lignites from the UK (Collinson et al., 2003; Pancost et al., 2007). Importantly, lignites are the lowest (maturity) rank of coal and have not experienced significant burial and associated temperature and pressure that leads to the loss of GDGTs (Schouten et al., 2004, 2013). Due to their low thermal maturity, lignites are thought to retain their original brGDGT distribution over geological timescales. For example, brGDGTs have been reported in an immature late Paleocene lignite from the USA (Weijers et al., 2011), early Eocene lignites from Germany (Inglis et al., 2017), as well as Miocene lignite from Germany (Stock et al., 2016). Although analyzed using the classical analytical method that did not separate 5- and 6-methyl brGDGTs, the brGDGT distribution in a late Paleocene lignite from North America is dominated by brGDGT-Ia (Weijers et al., 2011), similar to that seen in modern peats from the tropics and suggesting high terrestrial temperatures. This is consistent with our overall understanding of terrestrial climate during the greenhouse world of the late Paleocene and early Eocene (Huber and Caballero, 2011).

As the brGDGT distribution in peat deposits is dominated by production in the anoxic catotelm below the water

Table 1
brGDGT-based temperatures for Hani peatland.

Depth (cm)	Age (yr)	MBT$'_{5ME}$	MAT$_{mr}$ soil (RMSE 4.6 °C)	MAT$'_{5me}$ soil (RMSE 4.8 °C)	MAAT$_{peat}$ (RMSE 4.7 °C)
			De Jonge, 2014	De Jonge, 2014	This study
86	~700	0.53	6.6	10.9	4.5
102	~1000	0.53	6.6	11.3	4.8
838	~15,100	0.46	4.4	6.7	1.2
846	~15.400	0.39	2.8	5.4	−2.7
		Δ MAAT	3.0 °C	5.0 °C	5.4 °C

table where the seasonal temperature cycle is muted (see Section 4.1) brGDGT-based temperatures obtained from lignite deposits can be considered to reflect MAAT. We envision that future studies applying our new peat-specific calibrations to immature lignites will provide valuable new insights into terrestrial climate during the geological past. In addition, the GDGT concentrations in peats are generally much higher than those found in soils. We therefore propose that for studies of brGDGT distributions in (marine) sediments with a peat-dominated catchment area (e.g. Siberia (Frey and Smith, 2005)) or that contain independent evidence for the input of peat-derived material (e.g. high concentration of C_{31} αβ-hopanes or palynologic evidence for the input of typical peatland vegetation), the majority of GDGTs is likely derived from peatlands. In such settings it is more appropriate to use a peat-specific calibration rather than a mineral soil calibration.

5. CONCLUSIONS

Using 470 samples from 96 peatlands from around the world we explored the environmental controls on the bacterial brGDGT distribution in peats. We demonstrate that brGDGT distributions are correlated with peat pH and especially mean annual air temperature (MAAT). We develop for the first time peat-specific brGDGT-derived pH and temperature calibrations. In addition to their application in ancient peat-forming environments, we also suggest that these calibrations could be preferable to the available mineral soil calibration in marginal marine settings when it is clear that brGDGTs are predominantly derived from peats. We suggest caution in applying this proxy to late Holocene peat (e.g., covering the Medieval Climatic Anomaly and/or Little Ice Age) as both the calibration error and downcore variation appears to be larger than expected climate signals during this period. Taken together our results demonstrate that there is clear potential to use GDGTs in peatlands and lignites to reconstruct past terrestrial climate, opening up a new set of sedimentary archives that will help to improve understanding of the climate system during the geological past.

APPENDIX A. SUPPLEMENTARY DATA

Supplementary data associated with this article can be found, in the online version, at http://dx.doi.org/10.1016/j.gca.2017.01.038.

REFERENCES

Adcock R. J. (1878) A problem in least squares. *Analyst* **5**(2), 53–54.

Baird A. J., Milner A. M., Blundell A., Swindles G. T. and Morris P. J. (2016) Microform-scale variations in peatland permeability and their ecohydrological implications. *J. Ecol.* **104**(2), 531–544.

Baker A., Routh J. and Roychoudhury A. N. (2016) Biomarker records of palaeoenvironmental variations in subtropical Southern Africa since the late Pleistocene: Evidences from a coastal peatland. *Palaeogeogr. Palaeoclimatol. Palaeoecol.* **451**, 1–12.

Ballantyne A. P., Greenwood D. R., Sinninghe Damsté J. S., Csank A. Z., Eberle J. J. and Rybczynski N. (2010) Significantly warmer Arctic surface temperatures during the Pliocene indicated by multiple independent proxies. *Geology* **38**(7), 603–606.

Barber K. E. (1993) Peatlands as scientific archives of past biodiversity. *Biodivers. Conserv.* **2**(5), 474–489.

Burrows M. A., Fenner J. and Haberle S. G. (2014) Humification in northeast Australia: Dating millennial and centennial scale climate variability in the late Holocene. *Holocene* **24**(12), 1707–1718.

Chambers F. M. and Charman D. J. (2004) Holocene environmental change: contributions from the peatland archive. *Holocene* **14**(1), 1–6.

Chambers F. M., Booth R. K., De Vleeschouwer F., Lamentowicz M., Le Roux G., Mauquoy D. and Nichols J. E., et al. (2012) Development and refinement of proxy-climate indicators from peats. *Quatern. Int.* **268**, 21–33.

Chambers F. M., Brain S. A., Mauquoy D., McCarroll J. and Daley T. (2014) The 'Little Ice Age' in the Southern Hemisphere in the context of the last 3000 years: peat-based proxy-climate data from Tierra del Fuego. *Holocene* **24**(12), 1649–1656.

Chaves Torres L. and Pancost R. D. (2016) Insoluble prokaryotic membrane lipids in a *Sphagnum* peat: Implications for organic matter preservation. *Org. Geochem.* **93**, 77–91.

Collinson M. E., Hooker J. J. and Gröcke D. R. (2003) Cobham Lignite Bed and penecontemporaneous macrofloras of southern England: a record of vegetation and fire across the Paleocene-

Eocene Thermal Maximum. In *Causes and Consequences of Globally Warm Climates in the Early Paleogene* (eds. S. L. Wing, P. D. Gingerich, B. Schmitz and B. Thomas). Geological Society of America, Boulder, CO, pp. 333–349.

Cristea G., Cuna S. M., Fărcaş S., Tanţău I., Dordai E. and Măgdaş D. A. (2014) Carbon isotope composition as an indicator of climatic changes during the middle and late Holocene in a peat bog from the Maramureş Mountains (Romania). *Holocene* **24**, 15–23.

Dang X., Yang H., Naafs B. D. A., Pancost R. D., Evershed R. P. and Xie S. (2016) Direct evidence of moisture control on the methylation of branched glycerol dialkyl glycerol tetraethers in semi-arid and arid soils. *Geochim. Cosmochim. Acta* **189**, 24–36.

De Jonge C., Hopmans E. C., Stadnitskaia A., Rijpstra W. I. C., Hofland R., Tegelaar E. and Sinninghe Damsté J. S. (2013) Identification of novel penta- and hexamethylated branched glycerol dialkyl glycerol tetraethers in peat using HPLC–MS^2, GC–MS and GC–SMB-MS. *Org. Geochem.* **54**, 78–82.

De Jonge C., Hopmans E. C., Zell C. I., Kim J.-H., Schouten S. and Sinninghe Damsté J. S. (2014) Occurrence and abundance of 6-methyl branched glycerol dialkyl glycerol tetraethers in soils: implications for palaeoclimate reconstruction. *Geochim. Cosmochim. Acta* **141**, 97–112.

De Jonge C., Stadnitskaia A., Hopmans E. C., Cherkashov G., Fedotov A., Streletskaya I. D. and Vasiliev A. A., et al. (2015) Drastic changes in the distribution of branched tetraether lipids in suspended matter and sediments from the Yenisei River and Kara Sea (Siberia): Implications for the use of brGDGT-based proxies in coastal marine sediments. *Geochim. Cosmochim. Acta* **165**, 200–225.

Ding S., Xu Y., Wang Y., He Y., Hou J., Chen L. and He J. S. (2015) Distribution of branched glycerol dialkyl glycerol tetraethers in surface soils of the Qinghai-Tibetan Plateau: implications for brGDGTs-based proxies in cold and dry regions. *Biogeosciences* **12**(11), 3141–3151.

Frey K. E. and Smith L. C. (2005) Amplified carbon release from vast West Siberian peatlands by 2100. *Geophys. Res. Lett.* **32**(9), L09401.

Gallego-Sala A. V. and Prentice C. I. (2013) Blanket peat biome endangered by climate change. *Nat. Clim. Chang.* **3**(2), 152–155.

Gorham E., Janssens J. A. and Glaser P. H. (2003) Rates of peat accumulation during the postglacial period in 32 sites from Alaska to Newfoundland, with special emphasis on northern Minnesota. *Can. J. Bot.* **81**(5), 429–438.

Hansson S. V., Bindler R. and De Vleeschouwer F. (2015) Using peat records as natural archives of past atmospheric metal deposition. In *Environmental Contaminants* (eds. J. M. Blais, M. R. Rosen and J. P. Smol). Springer, Netherlands, pp. 323–354.

Hillel D. (1982) *Introduction to Soil Physics*. Academic Press, New York.

Hopmans E. C., Weijers J. W. H., Schefuß E., Herfort L., Sinninghe Damsté J. S. and Schouten S. (2004) A novel proxy for terrestrial organic matter in sediments based on branched and isoprenoid tetraether lipids. *Earth Plant. Sc. Lett.* **224**(1–2), 107–116.

Hopmans E. C., Schouten S. and Sinninghe Damsté J. S. (2016) The effect of improved chromatography on GDGT-based palaeoproxies. *Org. Geochem.* **93**, 1–6.

Huber M. and Caballero R. (2011) The early Eocene equable climate problem revisited. *Clim. Past* **7**(2), 603–633.

Huguet A., Fosse C., Laggoun-Défarge F., Toussaint M.-L. and Derenne S. (2010) Occurrence and distribution of glycerol dialkyl glycerol tetraethers in a French peat bog. *Org. Geochem.* **41**(6), 559–572.

Huguet A., Fosse C., Laggoun-Défarge F., Delarue F. and Derenne S. (2013) Effects of a short-term experimental micro-

climate warming on the abundance and distribution of branched GDGTs in a French peatland. *Geochim. Cosmochim. Acta* **105**, 294–315.

Huguet A., Francez A.-J., Jusselme M. D., Fosse C. and Derenne S. (2014) A climatic chamber experiment to test the short term effect of increasing temperature on branched GDGT distribution in *Sphagnum* peat. *Org. Geochem.* **73**, 109–112.

Inglis G. N., Collinson M. E., Riegel W., Wilde V., Farnsworth A., Lunt D. J. and Valdes P., et al. (2017) Mid-latitude continental temperatures through the early Eocene in western Europe. *Earth Plant. Sc. Lett.* **460**, 86–96.

Kaplan J. O., Bigelow N. H., Prentice I. C., Harrison S. P., Bartlein P. J., Christensen T. R. and Cramer W., et al. (2003) Climate change and Arctic ecosystems: 2. Modeling, paleodata-model comparisons, and future projections. *J. Geophys. Res. Atmos.* **108**(D19).

Kraemer B. M., Hook S., Huttula T., Kotilainen P., O'Reilly C. M., Peltonen A. and Plisnier P.-D., et al. (2015) Century-long warming trends in the upper water column of lake Tanganyika. *PLoS One* **10**(7), e0132490.

Lafleur P. M., Moore T. R., Roulet N. T. and Frolking S. (2005) Ecosystem respiration in a cool temperate bog depends on peat temperature but not water table. *Ecosystems* **8**(6), 619–629.

Laiho R. (2006) Decomposition in peatlands: Reconciling seemingly contrasting results on the impacts of lowered water levels. *Soil Biol. Biochem.* **38**(8), 2011–2024.

Lee K. E. (2007) Surface water changes recorded in Late Quaternary marine sediments of the Ulleung Basin, East Sea (Japan Sea). *Palaeogeogr. Palaeoclimatol. Palaeoecol.* **247**(1–2), 18–31.

Lei Y., Yang H., Dang X., Zhao S. and Xie S. (2016) Absence of a significant bias towards summer temperature in branched tetraether-based paleothermometer at two soil sites with contrasting temperature seasonality. *Org. Geochem.* **94**, 83–94.

Li J., Pancost R. D., Naafs B. D. A., Yang H., Zhao C. and Xie S. (2016) Distribution of glycerol dialkyl glycerol tetraether (GDGT) lipids in a hypersaline lake system. *Org. Geochem.* **99**, 113–124.

Liu X.-L., Leider A., Gillespie A., Gröger J., Versteegh G. J. M. and Hinrichs K.-U. (2010) Identification of polar lipid precursors of the ubiquitous branched GDGT orphan lipids in a peat bog in Northern Germany. *Org. Geochem.* **41**(7), 653–660.

Loomis S. E., Russell J. M. and Sinninghe Damsté J. S. (2011) Distributions of branched GDGTs in soils and lake sediments from western Uganda: implications for a lacustrine paleothermometer. *Org. Geochem.* **42**(7), 739–751.

Loomis S. E., Russell J. M., Eggermont H., Verschuren D. and Sinninghe Damsté J. S. (2014) Effects of temperature, pH and nutrient concentration on branched GDGT distributions in East African lakes: Implications for paleoenvironmental reconstruction. *Org. Geochem.* **66**, 25–37.

Mann M. E., Zhang Z., Rutherford S., Bradley R. S., Hughes M. K., Shindell D. and Ammann C., et al. (2009) Global signatures and dynamical origins of the little ice age and medieval climate anomaly. *Science* **326**(5957), 1256–1260.

Manuilova E., Schuetzenmeister A., and Model F. (2014) Method Comparison Regression. CRAN, https://cran.r-project.org/web/packages/mcr/index.html.

Mauquoy D., Yeloff D., Van Geel B., Charman D. J. and Blundell A. (2008) Two decadally resolved records from north-west European peat bogs show rapid climate changes associated with solar variability during the mid–late Holocene. *J. Quat. Sci.* **23**(8), 745–763.

McGlone M. S., Turney C. S. M., Wilmshurst J. M., Renwick J. and Pahnke K. (2010) Divergent trends in land and ocean

temperature in the Southern Ocean over the past 18,000 years. *Nat. Geosci.* **3**(9), 622–626.

McKenzie J. M., Siegel D. I., Rosenberry D. O., Glaser P. H. and Voss C. I. (2007) Heat transport in the Red Lake Bog, Glacial Lake Agassiz Peatlands. *Hydrol. Process* **21**(3), 369–378.

Menges J., Huguet C., Alcañiz J. M., Fietz S., Sachse D. and Rosell-Melé A. (2014) Influence of water availability in the distributions of branched glycerol dialkyl glycerol tetraether in soils of the Iberian Peninsula. *Biogeosciences* **11**(10), 2571–2581.

New M., Hulme M. and Jones P. (1999) Representing twentieth-century space-time climate variability. Part I: development of a 1961–90 mean monthly terrestrial climatology. *J. Climate* **12**(3), 829–856.

Nichols J. E., Booth R. K., Jackson S. T., Pendall E. G. and Huang Y. (2006) Paleohydrologic reconstruction based on *n*-alkane distributions in ombrotrophic peat. *Org. Geochem.* **37**(11), 1505–1513.

Pages 2k Consortium (2013) Continental-scale temperature variability during the past two millennia. *Nat. Geosci.* **6**(5), 339–346.

Pancost R. D., Baas M., van Geel B. and Sinninghe Damsté J. S. (2003) Response of an ombrotrophic bog to a regional climate event revealed by macrofossil, molecular and carbon isotopic data. *Holocene* **13**(6), 921–932.

Pancost R. D., Steart D. S., Handley L., Collinson M. E., Hooker J. J., Scott A. C. and Grassineau N. V., et al. (2007) Increased terrestrial methane cycling at the Palaeocene–Eocene thermal maximum. *Nature* **449**(7160), 332–335.

Pancost R. D., McClymont E. L., Bingham E. M., Roberts Z., Charman D. J., Hornibrook E. R. C. and Blundell A., et al. (2011) Archaeol as a methanogen biomarker in ombrotrophic bogs. *Org. Geochem.* **42**(10), 1279–1287.

Peterse F., Hopmans E. C., Schouten S., Mets A., Rijpstra W. I. C. and Sinninghe Damsté J. S. (2011) Identification and distribution of intact polar branched tetraether lipids in peat and soil. *Org. Geochem.* **42**(9), 1007–1015.

Peterse F., van der Meer J., Schouten S., Weijers J. W. H., Fierer N., Jackson R. B. and Kim J.-H., et al. (2012) Revised calibration of the MBT–CBT paleotemperature proxy based on branched tetraether membrane lipids in surface soils. *Geochim. Cosmochim. Acta* **96**, 215–229.

Peterse F., Martínez-García A., Zhou B., Beets C. J., Prins M. A., Zheng H. and Eglinton T. I. (2014) Molecular records of continental air temperature and monsoon precipitation variability in East Asia spanning the past 130,000 years. *Quaternary Sci. Rev.* **83**, 76–82.

Roland T. P., Daley T. J., Caseldine C. J., Charman D. J., Turney C. S. M., Amesbury M. J. and Thompson G. J., et al. (2015) The 5.2 ka climate event: Evidence from stable isotope and multi-proxy palaeoecological peatland records in Ireland. *Quat. Sci. Rev.* **124**, 209–223.

RStudio Team (2015) *RStudio: Integrated Development for R.* RStudio Inc, Boston, MA (USA).

Schellekens J., Bindler R., Martínez-Cortizas A., McClymont E. L., Abbott G. D., Biester H. and Pontevedra-Pombal X., et al. (2015) Preferential degradation of polyphenols from *Sphagnum* – 4-Isopropenylphenol as a proxy for past hydrological conditions in *Sphagnum*-dominated peat. *Geochim. Cosmochim. Acta* **150**, 74–89.

Schoon P. L., de Kluijver A., Middelburg J. J., Downing J. A., Sinninghe Damsté J. S. and Schouten S. (2013) Influence of lake water pH and alkalinity on the distribution of core and intact polar branched glycerol dialkyl glycerol tetraethers (GDGTs) in lakes. *Org. Geochem.* **60**, 72–82.

Schouten S., Hopmans E. C., Pancost R. D. and Sinninghe Damsté J. S. (2000) Widespread occurrence of structurally diverse tetraether membrane lipids: evidence for the ubiquitous presence of low-temperature relatives of hyperthermophiles. *Proc. Natl. Acad. Sci.* **97**(26), 14421–14426.

Schouten S., Hopmans E. C. and Sinninghe Damsté J. S. (2004) The effect of maturity and depositional redox conditions on archaeal tetraether lipid palaeothermometry. *Org. Geochem.* **35** (5), 567–571.

Schouten S., Hopmans E. C. and Sinninghe Damsté J. S. (2013) The organic geochemistry of glycerol dialkyl glycerol tetraether lipids: a review. *Org. Geochem.* **54**, 19–61.

Sinninghe Damsté J. S., Hopmans E. C., Pancost R. D., Schouten S. and Geenevasen J. A. J. (2000) Newly discovered non-isoprenoid glycerol dialkyl glycerol tetraether lipids in sediments. *Chem. Commun.* **17**, 1683–1684.

Sinninghe Damsté J. S., Schouten S., Hopmans E. C., van Duin A. C. T. and Geenevasen J. A. J. (2002) Crenarchaeol: the characteristic core glycerol dibiphytanyl glycerol tetraether membrane lipid of cosmopolitan pelagic crenarchaeota. *J. Lipid. Res.* **43**(10), 1641–1651.

Sinninghe Damsté J. S., Rijpstra W. I. C., Hopmans E. C., Weijers J. W. H., Foesel B. U., Overmann J. and Dedysh S. N. (2011) 13,16-Dimethyl octacosanedioic acid (*iso*-diabolic acid), a common membrane-spanning lipid of *Acidobacteria* subdivisions 1 and 3. *Appl. Environ. Microb.* **77**(12), 4147–4154.

Sinninghe Damsté J. S., Rijpstra W. I. C., Hopmans E. C., Foesel B. U., Wüst P. K., Overmann J. and Tank M., et al. (2014) Ether- and ester-bound iso-diabolic acid and other lipids in members of Acidobacteria subdivision 4. *Appl. Environ. Microb.* **80**(17), 5207–5218.

Sinninghe Damsté J. S. (2016) Spatial heterogeneity of sources of branched tetraethers in shelf systems: the geochemistry of tetraethers in the Berau River delta (Kalimantan, Indonesia). *Geochim. Cosmochim. Acta* **186**, 13–31.

Stanek W. (1973) Comparisons of methods of pH determination for organic terrain surveys. *Can. J. Soil Sci.* **53**(2), 177–183.

Stock A. T., Littke R., Lücke A., Zieger L. and Thielemann T. (2016) Miocene depositional environment and climate in western Europe: the lignite deposits of the Lower Rhine Basin, Germany. *Int. J. Coal. Geol.* **157**, 2–18.

Tierney J. E., Mayes M. T., Meyer N., Johnson C., Swarzenski P. W., Cohen A. S. and Russell J. M. (2010) Late-twentieth-century warming in Lake Tanganyika unprecedented since AD 500. *Nat. Geosci.* **3**(6), 422–425.

Tierney J. E., Schouten S., Pitcher A., Hopmans E. C. and Sinninghe Damsté J. S. (2012) Core and intact polar glycerol dialkyl glycerol tetraethers (GDGTs) in Sand Pond, Warwick, Rhode Island (USA): Insights into the origin of lacustrine GDGTs. *Geochim. Cosmochim. Acta* **77**, 561–581.

Väliranta M., Blundell A., Charman D. J., Karofeld E., Korhola A., Sillasoo Ü. and Tuittila E. S. (2012) Reconstructing peatland water tables using transfer functions for plant macrofossils and testate amoebae: a methodological comparison. *Quat. Int.* **268**, 34–43.

Vanneste H., De Vleeschouwer F., Martínez-Cortizas A., von Scheffer C., Piotrowska N., Coronato A. and Le Roux G. (2015) Late-glacial elevated dust deposition linked to westerly wind shifts in southern South America. *Sci. Rep.* **5**, 11670.

Vitt D. H., Bayley S. E. and Jin T.-L. (1995) Seasonal variation in water chemistry over a bog-rich fen gradient in Continental Western Canada. *Can. J. Fish. Aquat. Sci.* **52**(3), 587–606.

Weijers J. W. H., Schouten S., van der Linden M., van Geel B. and Sinninghe Damsté J. S. (2004) Water table related variations in the abundance of intact archaeal membrane lipids in a Swedish peat bog. *FEMS Microbiol. Lett.* **239**(1), 51–56.

Weijers J. W. H., Schouten S., Hopmans E. C., Geenevasen J. A. J., David O. R. P., Coleman J. M. and Pancost R. D., et al. (2006a) Membrane lipids of mesophilic anaerobic bacteria thriving in peats have typical archaeal traits. *Environ. Microbiol.* **8**(4), 648–657.

Weijers J. W. H., Schouten S., Spaargaren O. C. and Sinninghe Damsté J. S. (2006b) Occurrence and distribution of tetraether membrane lipids in soils: Implications for the use of the TEX$_{86}$ proxy and the BIT index. *Org. Geochem.* **37**(12), 1680–1693.

Weijers J. W. H., Schouten S., van den Donker J. C., Hopmans E. C. and Sinninghe Damsté J. S. (2007) Environmental controls on bacterial tetraether membrane lipid distribution in soils. *Geochim. Cosmochim. Acta* **71**(3), 703–713.

Weijers J. W. H., Panoto E., van Bleijswijk J., Schouten S., Rijpstra W. I. C., Balk M. and Stams A. J. M., et al. (2009) Constraints on the biological source(s) of the orphan branched tetraether membrane lipids. *Geomicrobiol. J.* **26**(6), 402–414.

Weijers J. W. H., Steinmann P., Hopmans E. C., Schouten S. and Sinninghe Damsté J. S. (2011) Bacterial tetraether membrane lipids in peat and coal: Testing the MBT-CBT temperature proxy for climate reconstruction. *Org. Geochem.* **42**(5), 477–486.

Woillard G. M. (1978) Grande Pile peat bog: A continuous pollen record for the last 140,000 years. *Quaternary Res.* **9**(1), 1–21.

Xiao W., Xu Y., Ding S., Wang Y., Zhang X., Yang H. and Wang G., et al. (2015) Global calibration of a novel, branched GDGT-based soil pH proxy. *Org. Geochem.* **89–90**, 56–60.

Xie S., Pancost R. D., Chen L., Evershed R. P., Yang H., Zhang K. and Huang J., et al. (2012) Microbial lipid records of highly alkaline deposits and enhanced aridity associated with significant uplift of the Tibetan Plateau in the Late Miocene. *Geology* **40**(4), 291–294.

Yang H., Lü X., Ding W., Lei Y., Dang X. and Xie S. (2015) The 6-methyl branched tetraethers significantly affect the performance of the methylation index (MBT') in soils from an altitudinal transect at Mount Shennongjia. *Org. Geochem.* **82**, 42–53.

Yvon-Durocher G., Allen A. P., Bastviken D., Conrad R., Gudasz C., St-Pierre A. and Thanh-Duc N., et al. (2014) Methane fluxes show consistent temperature dependence across microbial to ecosystem scales. *Nature* **507**(7493), 488–491.

Zell C., Kim J. H., Balsinha M., Dorhout D., Fernandes C., Baas M. and Sinninghe Damsté J. S. (2014) Transport of branched tetraether lipids from the Tagus river basin to the coastal ocean of the Portuguese margin: consequences for the interpretation of the MBT'/CBT paleothermometer. *Biogeosciences* **11**(19), 5637–5655.

Zheng Y., Li Q., Wang Z., Naafs B. D. A., Yu X. and Pancost R. D. (2015) Peatland GDGT records of Holocene climatic and biogeochemical responses to the Asian Monsoon. *Org. Geochem.* **87**, 86–95.

Zhou W., Zheng Y., Meyers P. A., Jull A. J. T. and Xie S. (2010) Postglacial climate-change record in biomarker lipid compositions of the Hani peat sequence, Northeastern China. *Earth Planet. Sci. Lett.* **294**(1–2), 37–46.

Zocatelli R., Jacob J., Gogo S., Le Milbeau C., Rousseau J. and Laggoun-Défarge F. (2014) Spatial variability of soil lipids reflects vegetation cover in a French peatland. *Org. Geochem.* **76**, 173–183.

Associate editor: Jaap Sinninghe Sinninghe Damste